FB100 Plasma Chemical Processes

Mgr. Ondřej Jašek, Ph.D.

jasek@physics.muni.cz

Outline

- Some general remarks about low temperature plasma applications

- Fullerenes, Diamond, Carbon nanotubes, Graphene

- Nanoparticle formation

Low temperature plasma overview

- The 2017 Plasma Roadmap: Low temperature plasma science and technology, I. Adamovich et al 2017 J. Phys. D: Appl. Phys. 50 323001 (46 pp)
- 1. New plasma sources and regimes
- 2. Plasma metamaterials and plasma photonic crystals
- 3. Multiphase plasmas
- 4. Particle transport in non-equilibrium plasmas
- 5. Plasma–surface interactions for material fabrication
- 6. Atomic layer processing
- 7. Plasma synthesis of nanomaterials and nanostructured materials
- 8. Plasma agriculture and innovative food cycles
- 9. Medical applications
- 10. Environmental applications
- 11. Plasma-assisted combustion and chemical conversion
- 12. Aerospace applications: propulsion and flow control
- 13. Thermal plasma applications
- 14. Plasma diagnostics
- 15. Plasmas in analytical chemistry
- 16. Plasma theory
- 17. Modelling and simulation
- 18. Atomic and molecular data for plasma science
- 19. Plasma chemistry: mechanisms, validation and distribution

Low temperature plasma overview

- 1. New plasma sources and regimes

  Plasmas sources in the spatial scale (such as the 1–1000 μm domain of microplasmas) or the temporal scale (sub-50 ns electrical or optical excitation, transitory plasmas and nanosecond pulsed discharges)

  Confining the plasmas to such small space and time can lead to new regimes and phases – high density phases such as supercritical fluids.

  There is potential for microplasma reactors to be patterned completely onto a chip.
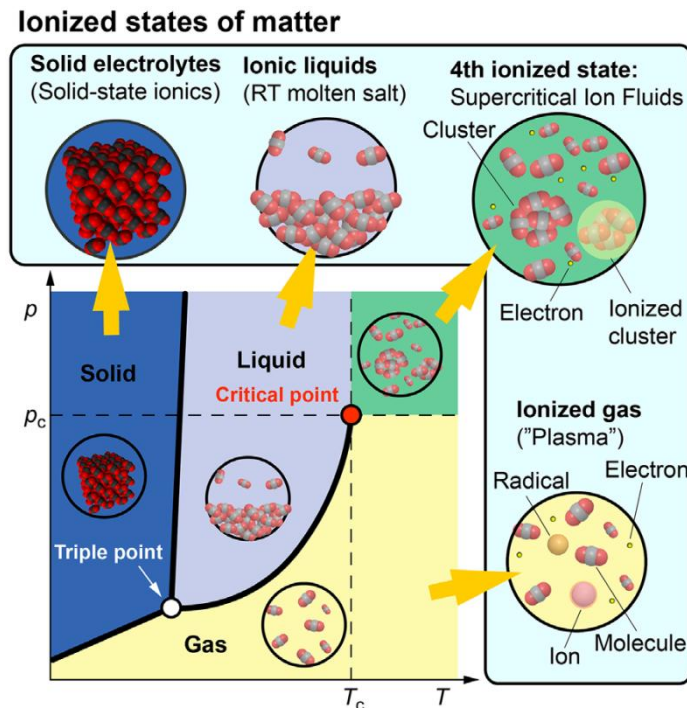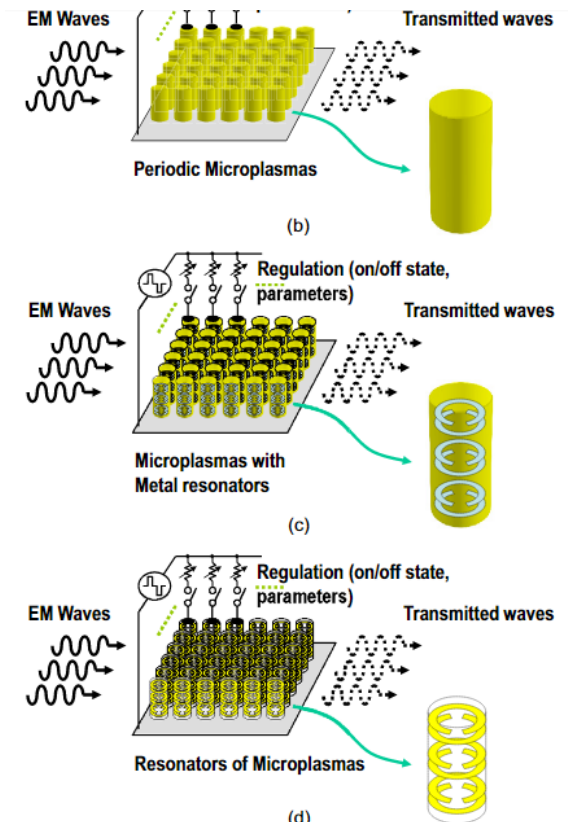
Low temperature plasma overview

- 2. Plasma metamaterials and plasma photonic (PC) crystals

Metamaterials have structures ('atoms') that are subwavelength in scale. Interactions arise through resonances within the structures—conduction electrons (in metallic structures) or bound electrons (in dielectric structures). Quasi-homogenous effective permittivity (ε_{eff}) or permeability (μ_{eff}) can become negative in plasma! In contrast, PCs respond by exploiting successive Bragg scattering and interferences at interfaces that make up the structure. Gaseous plasmas consisting of electrons and ions afford the possibility of serving as reconfigurable resonating elements in MMs and as scattering elements in PCs.


$$\varepsilon_{\mathrm{p}} = 1 - \frac{\omega_{\mathrm{pe}}^2}{\omega^2 (1 + j\nu_{\mathrm{m}}/\omega)} = 1 - \frac{e^2 n_{\mathrm{e}}}{\varepsilon_0 m_{\mathrm{e}} \omega^2 (1 + j\nu_{\mathrm{m}}/\omega)}, \quad (1)$$

Low temperature plasma overview

- ## 3. Multiphase plasmas

  High density of liquids leads to increased collision frequency can enable discharge dynamics at the sub-nanosecond time scale with spatial gradients in narrow discharge filaments. Plasmas can be electrically produced but also induced by lasers. Focus is on gas-liquid interface such as bubbles. Most research is focused on aqueous solutions but also hydrocarbon liquids are studied – fuels and materials. Traditional application in analytical chemistry, nanoparticle and coatings preparation – plasma spraying. Possible new use in environmental remediation, disinfection, medical and agricultural applications. Challenging control of plasma-induced liquid phase chemistry - advective to diffusive transport, enhanced liquid and charge injection into the plasma, two-way interaction between liquid and gas phase.
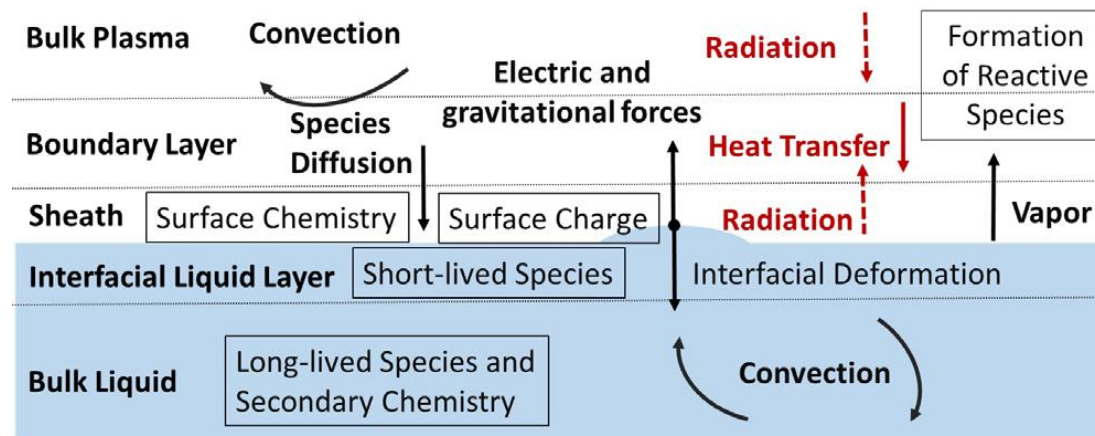
Low temperature plasma overview
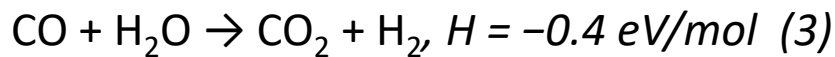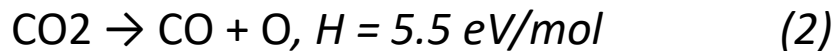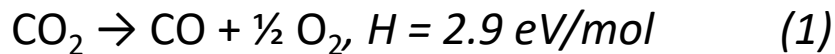# - theory, modelling, diagnostics

- 4. Particle transport in non-equilibrium plasmas – Boltzmann's equation and Monte Carlo simulations are used to describe charged particles in low pressure. There is a need to expand those to charged particles with variable mass, multiple scattering and transport in liquids and high pressure. Special interest is given to high reduced electric fields phenomena including streamers , ionization waves and high energy electrons.

- 14. Plasma diagnostics - laser methods

- 16. Plasma theory

- 17. Modelling and simulation

- 18. Atomic and molecular data for plasma science – cross sections, reaction schemes, errors

- 19. Plasma chemistry: mechanisms, validation and distribution

Low temperature plasma overview

- 5. Plasma–surface interactions for material fabrication

- 6. Atomic layer processing – Plasma-enhanced ALD – wide range of reactions, PE ALE atomic layer etching – source of radicals and directionality , Si_3N_4, Si, SiO_2

- 7. Plasma synthesis of nanomaterials and nanostructured materials

- 8. Plasma agriculture and innovative food cycles

- 9. Medical applications – need of deeper understanding of interaction of plasma species with living enviroment

- 10. Environmental applications - atmospheric pressure non-thermal plasma, in past focused to ozone generation and electrostatic precipitatio. Currently focused on exhaust gases and conversion of CO_2, CH_4 and syngas into value-added products, such as hydrogen and hydrocarbons.

- 11. Plasma-assisted combustion and chemical conversion

- 12. Aerospace applications: propulsion and flow control – Hall engines, but also general interactions of plasma with magnetic fields – plasma reconnection, spokes

- 13. Thermal plasma applications - arc welding, plasma cutting and plasma spraying

- 15. Plasmas in analytical chemistry – ICP and new plasma sources – laser-induced breakdown spectroscopy (LIBS) and laser-assisted molecular emission spectrometry (LAMIS)

11. Plasma-assisted combustion and chemical conversion - CO_2 dissociation

$CO_2 \rightarrow CO + \frac{1}{2} O_2$, $H = 2.9\ eV/mol$ (1)

$CO2 \rightarrow CO + O$, $H = 5.5\ eV/mol$ (2)

$CO + H_2O \rightarrow CO_2 + H_2$, $H = -0.4\ eV/mol$ (3)

$\eta = H/E_{CO}$ (4)

CO_2 dissociation is an important process in CO_2 lasers and can be stimulated with high efficiency with vibration excitation. It is model case for similar "oxides" molecules and their reduction. And its related to CO_2 mitigation in exhaust gases, industrial synthesis of fuel related applications and possible future hydrogen production on Mars.
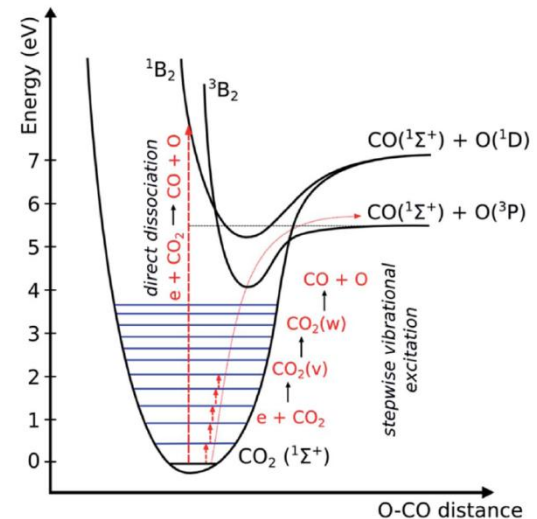

Fig. 7 Schematic diagram of some CO_2 electronic and vibrational levels, illustrating that much more energy is needed for direct electronic excitation–dissociation than for step-wise vibrational excitation, i.e., the so-called ladder climbing process.

A. Fridman, Plasma Chemistry, Chapter 5, Cambridge University Press, 2008

CO$_2$ dissociation

Thermal plasma systems such as electric arcs or high-pressure RF discharges provide CO$_2$ dissociation by a high-temperature shift of thermodynamic equilibrium in the direction of product formation. It can be seen from Fig. 5–3 that significant CO$_2$ dissociation requires plasma temperatures of about 2500–3000 K in conditions of thermodynamic quasi equilibrium. Plasma in this case is only a heater – a provider of the required high temperature. a) The products of decomposition (1) generated at high temperature (Fig. 5–3), CO and oxygen, can be protected from reverse reactions only by quenching, that is, by fast non-adiabatic cooling. If the products escape from the hot plasma zone too slowly, the thermodynamic quasi equilibrium is continuously sustained during the temperature decrease and products can be converted back to CO$_2$. Quenching (cooling rate) 10^7–10^8 K/s. b) Absolute quenching of the CO$_2$ dissociation requires a cooling process sufficient to save all CO formed in the quasi-equilibrium high-temperature zone. As a result the maximum energy efficiency value of CO$_2$ dissociation in quasi-equilibrium thermal plasmas is only 43%.

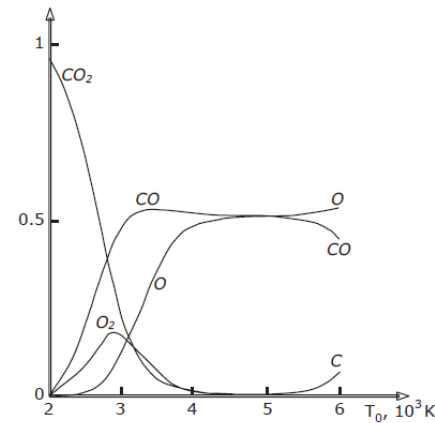➜ **Higher efficiency can only be reached in non-equilibrium plasma systems**

Figure 5–3. Equilibrium molar fraction of products of CO$_2$ decomposition in thermal plasma as function of temperature in hot discharge zone at fixed gas pressure $p = 0.16$ atm.
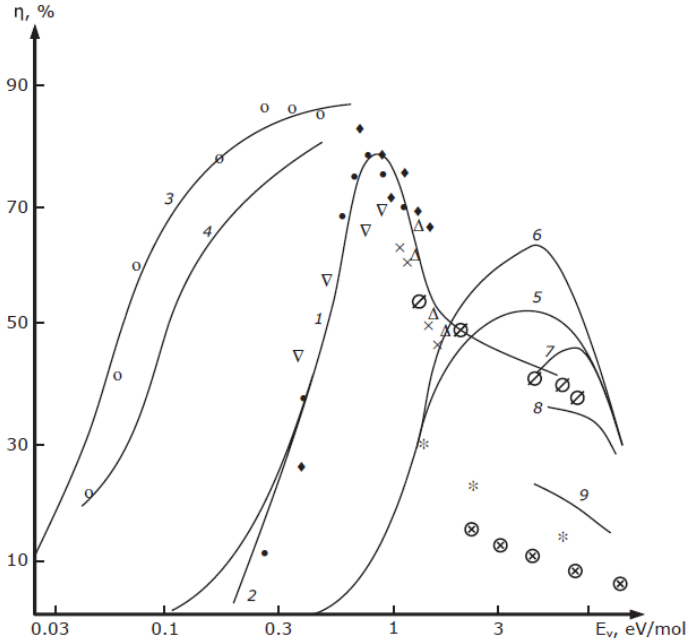
CO$_2$ dissociation

Figure 5–2. Energy efficiency of CO$_2$ dissociation as a function of specific energy input. (1, 2), non-equilibrium calculations in one- and two-approximations; non-equilibrium calculations for supersonic flows: (3) M = 5; (4) M = 3.5; calculations of thermal dissociation with (5) ideal and (6) super-ideal quenching; (7) thermal dissociation with quenching rates 10^9 K/s, (8) 10^8 K/s, (9) 10^7 K/s. Different experiments in microwave discharges: o, ♦, Δ, ×. Experiments in supersonic microwave discharges: ●. Experiments in different RF-CCP discharges: o, ∇. Experiments in RF-ICP discharges: ∅. Experiments in different arc discharges: ⊗, *.
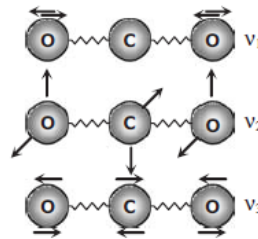

Figure 5–11. Vibrational modes of CO$_2$ molecules: ν_1, symmetric valence vibrations; ν_2, double degenerate symmetric deformation vibrations; ν_3, asymmetric valence vibrations.
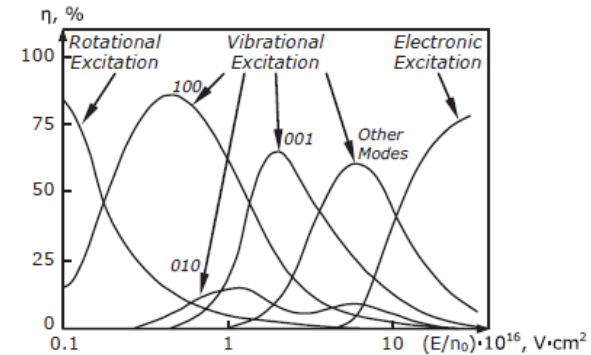
Figure 5–5. Fractions of non-thermal CO$_2$ discharge energy transferred from plasma electrons to different channels of excitation of the molecule.

CO$_2$ dissociation

The most common types of plasma used for CO$_2$ conversion are dielectric barrier discharges (DBDs), microwave (MW) plasmas and gliding arc (GA) discharges. The highest energy efficiency was reported for a MW plasma, i.e., up to 90% but this was under very specific conditions, i.e., supersonic gas flow and reduced pressure (100–200 Torr), and a pressure increase to atmospheric pressure, which would be desirable for industrial applications, yields a dramatic drop in energy efficiency. Indeed, at normal flow conditions and atmospheric pressure, an energy efficiency up to 40% was reported. A GA plasma also exhibits a rather high energy efficiency, even at atmospheric pressure, i.e., around 43% for a conversion of 18% in the case of CO$_2$ splitting.

The energy efficiency of a DBD is more limited, i.e., in the order of 2–10%, but as demonstrated already for other applications, it should be possible to improve this energy efficiency by inserting a (dielectric) packing into the reactor, i.e., a so-called packed bed DBD reactor.

Adding catalytic functionality should enable further improvement in conversion efficiency and selectivity of final products.

A. Bogart, T. Kozak, K. van Laer, R. Snoeckx, Plasma-based conversion of CO2: current status and future challenges, Faraday Discuss., 2015, 183, 217.

A. Ozkan, T. Dufour, T. Silva, N. Britun, R. Snyders, F. Reniers and A. Bogaerts, DBD in burst mode: solution for more efficient CO2 conversion, Plasma Sources Sci. Technol. 25 (2016) 055005 (9pp).

G. Chena, V. Georgieva, T. Godfroid, R. Snyders ,M.-P. Delplancke-Ogletree, Plasma assisted catalytic decomposition of CO2, Applied Catalysis B: Environmental 190 (2016) 115–124.

T. Nunnally, K. Gutsol, A. Rabinovich, A. Fridman, A. Gutsol and A. Kemoun, Dissociation of CO2 in a low current gliding arc plasmatron, J. Phys. D: Appl. Phys. 44 (2011) 274009 (7pp).
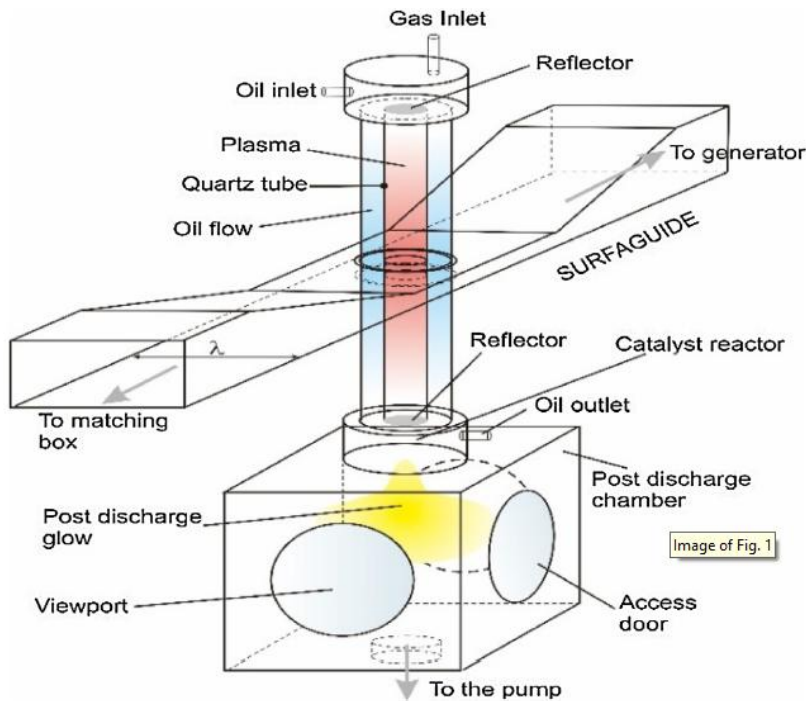
CO$_2$ dissociation

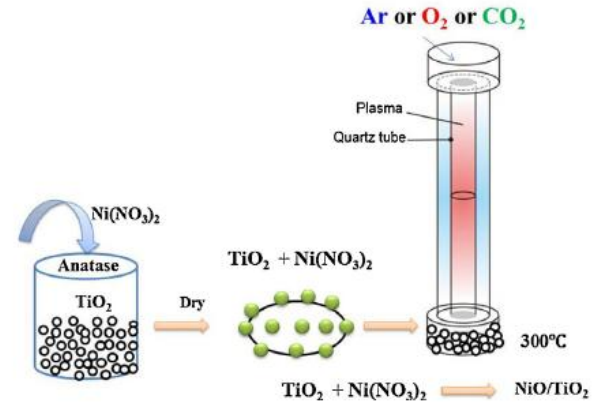Fig. 1. Schematic representation of surface-wave microwave set-up.

Fig. 2. Schematic representation of catalyst preparation by impregnation and plasma treatment methods.

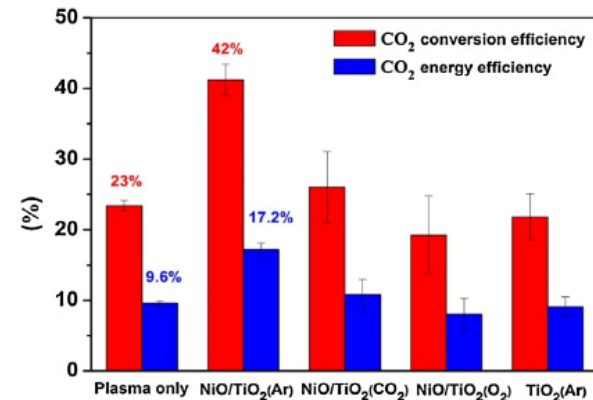Fig. 7. CO$_2$ conversion and energy efficiencies, measured during the plasma-catalysis CO$_2$ dissociation, are shown for the NiO/TiO$_2$ catalysts prepared by plasma treatment with different gases (O$_2$, Ar, CO$_2$).

G. Chena, V. Georgieva, T. Godfroid, R. Snyders ,M.-P. Delplancke-Ogletree, Plasma assisted catalytic decomposition of CO2, Applied Catalysis B: Environmental 190 (2016) 115–124.
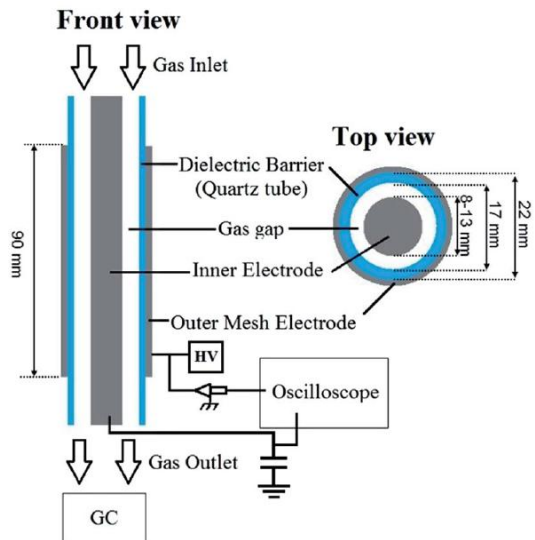
CO$_2$ dissociation

Front view

Gas Inlet

Top view

Dielectric Barrier (Quartz tube)

Gas gap

Inner Electrode

Outer Mesh Electrode

90 mm

17 mm

22 mm

8-13 mm

HV

Oscilloscope

Gas Outlet

GC

Fig. 1 Schematic diagram of the experimental setup, in front view and top view.

CO$_2$ (100) (020) — CO$_2$ (010) — CO$_2$ (001) — sum of higher vibrations — sum of all vibrations — Electronic excitation — Dissociation — Ionization
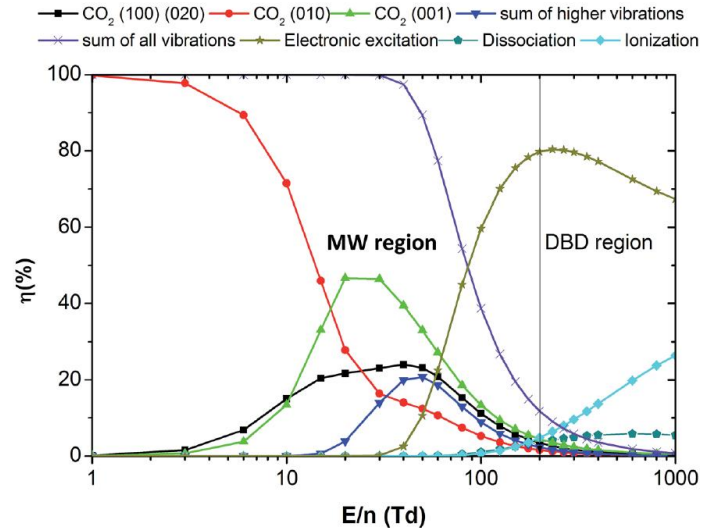
η(%)

MW region

DBD region

E/n (Td)

Fig. 4 The fraction of electron energy transferred to different channels of excitation as well as ionization and dissociation of CO$_2$, as a function of the reduced electric field (E/n), as calculated from the corresponding cross sections of the electron impact reactions. The E/n region characteristic for MW plasma and DBD plasma are indicated.
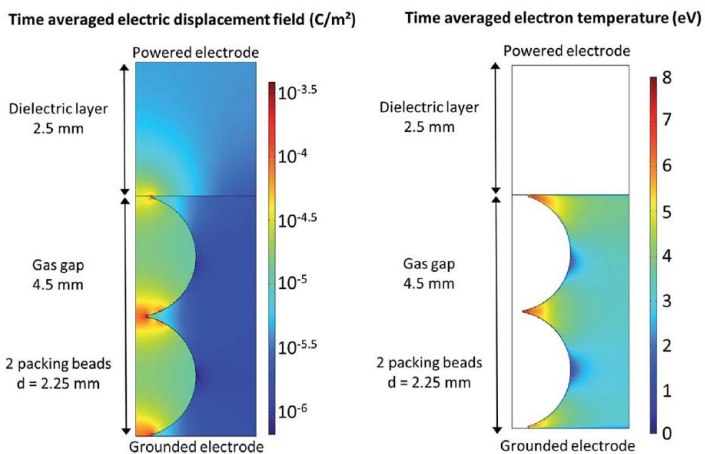
Time averaged electric displacement field (C/m²)

Powered electrode

Dielectric layer 2.5 mm

Gas gap 4.5 mm

2 packing beads d = 2.25 mm

$10^{-3.5}$
10^{-4}
$10^{-4.5}$
10^{-5}
$10^{-5.5}$
10^{-6}

Grounded electrode

Time averaged electron temperature (eV)

Powered electrode

Dielectric layer 2.5 mm

Gas gap 4.5 mm

2 packing beads d = 2.25 mm

Grounded electrode

Fig. 9 Calculated time averaged electric displacement field and electron temperature over one period of the applied potential.

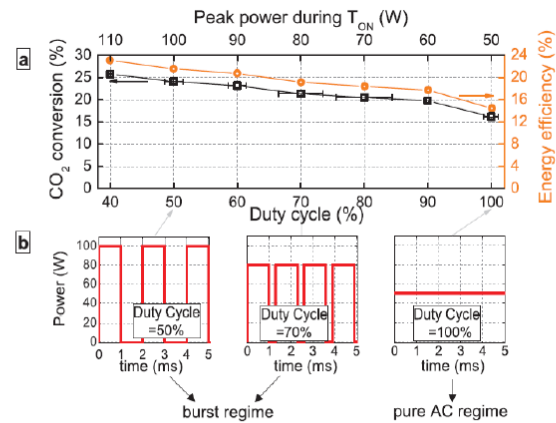Peak power during T$_{ON}$ (W)

a

CO$_2$ conversion (%)

Energy efficiency (%)

Duty cycle (%)

b

Power (W)

Duty Cycle =50%

Duty Cycle =70%

Duty Cycle =100%

time (ms)

burst regime

pure AC regime

Figure 4. (a) CO$_2$ conversion and energy efficiency as a function of the duty cycle — $P_{applied}$ = 50 W, f_{signal} = 28.6 kHz, $f_{repetition}$ = 400–900 Hz and $\Phi(CO_2)$ = 200 mL$_n$ · min^{-1}; (b) power versus time for D_{Cycle} = 50, 70 and 100%.

A. Bogart, T. Kozak, K. van Laer, R. Snoeckx, Plasma-based conversion of CO2: current status and future challenges, Faraday Discuss., 2015, 183, 217.
A. Ozkan, T. Dufour, T. Silva, N. Britun, R. Snyders, F. Reniers and A. Bogaerts, DBD in burst mode: solution for more efficient CO2 conversion, Plasma Sources Sci. Technol. 25 (2016) 055005 (9pp).